Volumetric Imaging of Cardiac Current Sources using Lp-Norm Regularization

Azar Rahimi[1], Jingjia Xu[1], John R Fitz-Clarke[2], Linwei Wang[1]

[1] Rochester Institute of Technology, Rochester, USA
[2] Dalhousie University, Halifax, Canada

Abstract

Computational cardiac current source imaging aim to mathematically reconstruct current source activities from noninvasive voltage data sensed on the body-surface. However, the progress in this field is hindered by the ill-posedness and the lack of a unique solution of the reconstruction problem. Common $L2$ and $L1$-norm regularization tend to produce a solution that is either too diffused or too scattered to reflect the complex spatial structure of current source distribution in the heart. In this work, we propose a general regularization with Lp-norm $(1 < p < 2)$ constraint to bridge the gap and balance between an overly-smeared and overly-focal solution in cardiac source reconstruction. In a set of phantom experiments, we demonstrate the superiority of the proposed Lp-norm method over its $L1$ and $L2$ counterparts in imaging cardiac current sources with increasing extents. Through computer-simulated as well as real-data experiments, we further demonstrate the feasibility of the proposed method in imaging the complex structure of current sources activity along the infarct border. This ability to preserve the spatial structure of source distribution is important for revealing the potential disruption to the normal current flow in the heart.

1. Introduction

Electrical currents in the heart work as bioelectric sources to produce bioelectromagnetic fields that can be sensed as small voltages in the volume conductor of the torso. This voltage change over time is measured on the body-surface as electrocardiograms (ECG). Biophysical models of this bioelectrical field can be derived from the *quasi-static electromagnetism* [1] where the ECG measurements $\mathbf{b}$ are described as linear combination of the spatial distribution of current source $\mathbf{v}$: $\mathbf{b} = \mathbf{H}\mathbf{v}$.

Because there is a lack of experimental techniques to physically measure cardiac electrical signals deep into the thickness of the myocardium, many computational strategies are developed which aim to mathematically *reconstruct* the 3-dimensionally distributed, time-varying bioelectrical currents by solving this inverse problem, using noninvasive signals collected at different body-surface locations. However, this inverse problem suffers from both mathematical and physical ill-posedness. The mathematical ill-posedness is caused by the limited number of field measurements compared to the large degree of freedom in the possible location of current sources. The physical ill-posedness is unique to the underlying biophysics of this problem: even with *virtually* continuous measurements on the surface, different configurations of 3D sources may produce the same surface measurements [1]. Therefore, if the solution is sought transmurally, this inverse problem is intrinsically ill-posed without a unique solution in its most unconstrained form. Proper assumptions of the solutions must be made in order to guarantee a unique solution.

The most commonly used approach is to restrain the solution on the epicardium [2] and/or endocardium [3], sacrificing the information into the depth of the myocardium in exchange for a unique solution. There are few successes in *imaging* the cardiac electrical sources deep into the myocardium, which often involve complex, physiological prior knowledge from computational electrical propagation models of the heart [4, 5]. Although these methods provide volumetric imaging of cardiac electrical dynamics, the quadratic regularization used in these methods conflict with the complex structural properties of the cardiac current sources. The question is: *what is the obstacle that hinders the progress of cardiac source reconstruction towards a volumetric solution?* We hypothesize that this is, at least in part, caused by the unique spatial property of cardiac current sources. Cardiac current sources undergo a complex spatio-temporal evolution process in each cardiac cycle, starting from a few focal sites and then propagating throughout the myocardium. In a healthy heart, the current sources form an *excitation* and *repolarization* wavefront during depolarization and repolarization stages, separating active and resting cells (Fig 1 A). At the end of depolarization and before the state of repolarization, the healthy heart goes through a stage without current flow (ST-segment in an ECG cycle)while in an infarcted heart, active current sources will be concentrated along the infarct border, as shown in Fig 1B. These time-varying spatial structure of

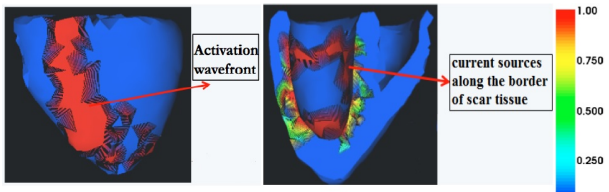

(A) Healthy heart (B) Infarcted heart

Figure 1. Illustration of the spatial structure of ventricular current sources during a healthy (A) or pathological (B) cardiac cycle.

the current source is important because it reveals the potential disruption to a normal current flow.

This unique spatial property of cardiac current sources decides that $L2$ or $L1$ regularization will produce a solution that is either too smeared or too focal to reveal the underlying source activity. Based on this observation, we propose a general regularization with Lp-norm $(1 < p < 2)$ constraint to cardiac source reconstruction. Balancing between a smeared and a focal solution, Lp-norm constraint bridges the gap between $L1$ and $L2$-norm regularization. The nonlinear Lp-norm regularization is solved after being cast to second-order cone programming (SOCP) problem. In a set of phantom experiments, the proposed method is shown to outperform its $L1$ and $L2$ counterparts in imaging cardiac current sources with increasing extents. Through computer-simulated as well as real-data experiments, we further demonstrate the feasibility of the proposed method in imaging the complex structure of current sources distributed along the infarct border.

2. Methodology

The quasi-static electromagnetism [1] explains the relation between the potential distribution within the torso volume and the cardiac current sources as:

$$\sigma_{blk}\nabla^2\phi_e(\mathbf{r}) = \nabla\cdot(-\mathbf{D_{int}}v(\mathbf{r})),\ \forall \mathbf{r}\in\mathbf{\Omega_h} \quad (1)$$

$$\sigma\nabla^2\phi(\mathbf{r}) = 0,\ \forall \mathbf{r}\in\mathbf{\Omega_{t/h}} \quad (2)$$

where the Poisson equation (1) describes, on a bidomain heart model, how the extracellular potential ϕ_e within the heart volume Ω_h originates from the current sources $\mathbf{D_{int}}v$ where v is the targeted solution that represents the gradient of the action potential and $\mathbf{D_{int}}$ is the anisotropic intracellular conductivity tensor that can be obtained by fiber structure mapper from literature data[6]. σ_{blk} is the isotropic bulk conductivity. The Laplace equation (2) describes, on the monodomain torso model, how the potential ϕ distributes within the torso volume $\Omega_{t/h}$ external to the heart with conductivity σ. It has been previously shown that, using proper numerical methods such as mesh-free and boundary element methods, one can numerically solve equations (1,2) on a subject heart-torso model, and obtain linear relationship: $\mathbf{b} = \mathbf{Hv}$ [7].

Lp-Norm Regularization. As mentioned earlier, reconstructing 3D current sources from ECG data is a highly ill-posed inverse problem with non-unique solutions in its most unconstrained form. However, complex spatial distribution of cardiac current sources conflicts with a focal $L1$ or smooth $L2$ constraint. To estimate the special structure of current sources we apply Lp-norm regularization:

$$\min_{\mathbf{v}} ||\mathbf{b}-\mathbf{Hv}||_{\mathbf{2}}^{\mathbf{2}} + \lambda||\mathbf{v}||_{\mathbf{p}}, ||\mathbf{v}||_{\mathbf{p}} = (\sum_{\mathbf{i=1}}^{\mathbf{n}}[\mathbf{v_i}]^{\mathbf{p}})^{\mathbf{1/p}} \quad (3)$$

where $1 < p < 2$ and n is the dimension of $\mathbf{v}$, *i.e.,* the number of mesh-free nodes used to represent the ventricular myocardium.

Lp-norm penalty term promotes different forms of structural sparsity as often observed in the heart. It offers the potential to outperform sparse $L1$-norm and diffuse $L2$-norm for localizing sources with different extents/sizes. Adopting second-order cone programming (SOCP), we convert regularization (3) to SOCP problem and solve it.

3. Experiments and results

3.1. Computer-simulated experiments

We consider synthetic experiments on an image-derived human heart-torso model. The torso surface is represented by triangulated elements with 370 vertices. The ventricular myocardium is represented by 1019 evenly distributed nodes. To take into account the complex spatial shape of the source distribution, the accuracy of 3D source estimation is evaluated using the *source overlap (SO)* defined as the ratio of the intersection to the union between the estimated and the *true* current sources. We also perform comparison studies of the proposed Lp-norm method with $L1$ and $L2$-norm methods in 3D source imaging.

Value of p vs. Source Extent. In the first set of experiments, we investigate the performance of Lp-norm regularization in localizing current sources with different sizes. In total, 44 settings are studied, considering a region of active current sources sized from 1% to 45% of LV. These sources form a region with structural sparsity located randomly inside the ventricular myocardium. The nodes lying within the region of active sources are assigned with values 1, while the rest of the ventricular nodes are set to be 0. For each setting, the corresponding ECG measurements are simulated on the 370 vertices on the body-surface, and are corrupted with noise (20 dB SNR) before being input to the Lp-norm method to reconstruct the region of active current sources. For every source setting, Lp-norm estimation is obtained using $p \in \{1.1, 1.3, 1.5, 1.7, 1.9\}$, and is compared to that obtained by $L1$ and $L2$ solutions.

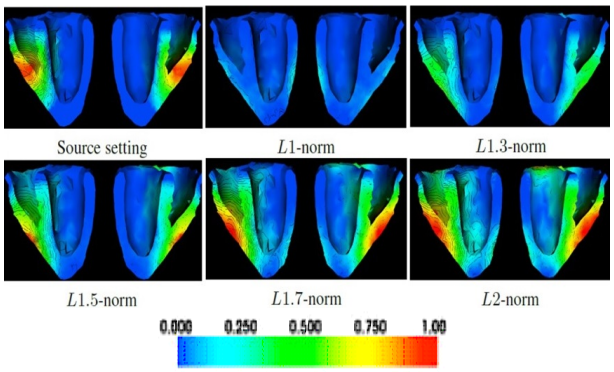

Figure 2. Source estimation using Lp-norm regularization for $1 \leq p \leq 2$. Active sources are located close to the right ventricle apex. Increasing the p value increases the source extent such that $L1$-norm obtains too scattered source distribution while $L2$-norm provides overly-diffused solution. Current magnitudes are normalized to 1.

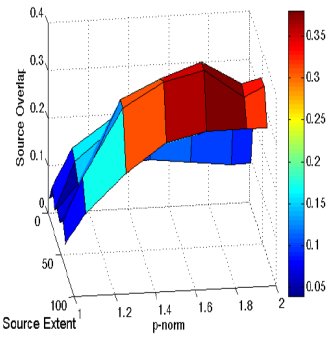

Figure 3. Source overlap (SO, vertical axis) obtained by Lp-norm reconstruction ($1 \leq p \leq 2$, horizontal axis 1) for active sources with different extents (from 1% to 45% of LV, horizontal axis 2).

Fig 2 shows an example of source estimation using Lp-norm regularization for $1 \leq p \leq 2$, where the active current sources are located close to the right ventricle apex. The $L1$-norm estimation of active sources results in a very sparse source reconstruction (SO = 0.07) scattered in the *true* region of active sources. Increasing the p value for the Lp-norm regularization, the detected source extent increases. At $p = 1.7$, we obtain an accurate estimation of source extent (SO = 0.33), which is located very close to the *true* region of active sources. As p continues to increase, the estimated source region becomes more extended but still has a relatively compact center. There is a sudden change of pattern in the solution when p equals to 2, where the estimated source region ($L2$ solution) becomes very diffused (SO = 0.25).

Fig 3 summarizes the mean SO (vertical-axis) between the *true* and estimated source region obtained using Lp-norm regularization, as p increases from 1 to 2 (horizontal axis 1) and as the size of active region increases (horizontal axis 2). As shown, for source regions of all sizes, similar trend of SO change can be observed as p increases from 1 to 2 in the Lp-norm regularization. The sparse solution produced by $L1$-norm regularization, though produces low false-positives, also has a high under-estimation and therefore a low value of SO. On the other extreme, the smeared solution of $L2$-norm regularization, though is able to detect the majority of the *true* active sources, tends to have a high over-estimation and thus leads to again a low SO value. Therefore, for source region of all sizes, we can observe an increase followed by a decrease of the SO value when p increases from 1 to 2, with the maximum SO obtained when $1.5 \leq p \leq 1.7$.

For all the 44 cases, the mean and standard deviation of SO are 0.36 ± 0.05 compared to $L1$ and $L2$ with mean and standard deviation 0.06 ± 0.03 and 0.30 ± 0.07, respectively. Paired students t-test shows that the accuracy of the proposed method in preserving the structure of the infarct border is significantly higher than that of $L1$-norm ($p < 0.0001$) and $L2$-norm ($p < 0.001$).

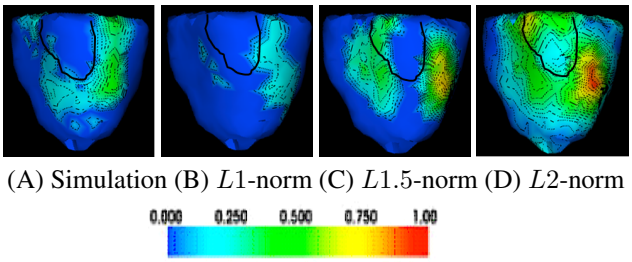

(A) Simulation (B) $L1$-norm (C) $L1.5$-norm (D) $L2$-norm

Figure 4. Estimation of current sources activity along the infarct border using Lp vs. $L1$ and $L2$-norm counterparts.

Imaging Source Activity along the Infarct Border. In this set of experiments, we increases the complexity of the experimental settings and consider *realistic* structures of current sources, which are generated based on the Aliev-Panfilov [8] model, of the spatio-temporal propagation of electrical waves in the ventricles. Therefore, we examine the feasibility of the proposed method in estimating current source activity along the infarct border during the ST-segment of an ECG cycle (Fig 1 B).

Fig 4 shows an example of current source distributed along the infarct border that extends from basal to mid anterior and anterolateral LV. Lp regularization ($p = 1.5$) solution reports SO = 0.35. In comparison, the $L1$ regularization produces a scattered solution (SO = 0.08) and the $L2$ regularization produces a diffused solution (SO = 0.26), neither of which is able to capture the structure of the current sources along the infarct border. This ability of the proposed Lp-norm to faithfully reconstruct the current sources activity along the infarct border is of great importance, since the infarct border is the common site for triggered

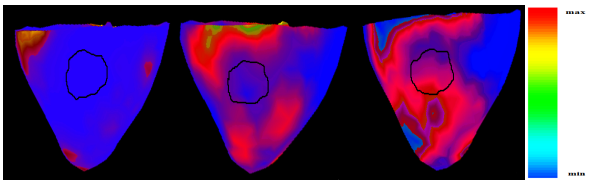

(A) $L1$-norm (B) $L1.5$-norm (C) $L2$-norm

Figure 5. Estimation of current source activity along the infarct border using Lp, $L1$ and $L2$-norm regularizations for a post-infarction human subject.

electrical activity and re-entrant circuits that can initiate and maintain life-threatening ventricular arrhythmia.

3.2. Real-data experiments

Because of the important therapeutic value of infarct border, and the promising results obtained from our initial synthetic experiments, we conduct an initial real-data experiment on a real post-infarction human subject, to assess the feasibility of the proposed Lp-norm method in detecting current source activity along the infarct border.

Experimental data were collected from a patient with prior myocardial infarction and made available to this study by *2007 PhysioNet / Computers in Cardiology Challenges* [9]. MRI scan of the patient has 8-mm inter-slice spacing and 1.33 mm/pixel in-plane resolution. Body-surface ECG maps were recorded by *Dalhousie University* standards [10] at 123 known anatomical sites and interpolated to 370 nodes of the *Dalhousie* torso model; each BSP recording consists of a single averaged PQRST complex sampled at 2k Hz. Gold standards of the infarct were provided by cardiologists who examined the late Gadolinium enhanced (LGE) MR scans of the patient, and were provided in terms of the location and size of the infarct with regard to the 17-segment division of the LV according to AHA standards [11]. Specifically, according to the gold standard, the infarct center is located at segment 10 and 11, between mid-inferior and mid-inferolateral of the subject's left ventricle (highlighted with black contour on Fig 5). ECG data collected at the $192ms$ during the ST-segment are selected as the input data.

As shown in Fig 5, $L1$ regularization results in a very sparse solution scattered far from the infarct center while $L2$ solution is diffused and covers the infarct center, *i.e.,* the structure of the infarct border can not be discerned by the reconstruction. The proposed Lp method ($p = 1.5$) provides a more accurate estimation of the current source activity around the center of the infarct.

4. Conclusions

The inverse problem of cardiac source reconstruction is notoriously ill-posed without a unique solution. Progress towards 3D cardiac source reconstruction is further hindered by the complex structure of current source distribution in the heart, because of which the common $L1$ and $L2$-norm constraints are no longer proper. We propose a general Lp-norm regularization to bridge the gap between $L1$ and $L2$ regularization in imaging cardiac current source distributions that are of important therapeutic information.

Our experimental results show that the optimal solutions are obtained at $p = 1.5 - 1.7$ for sources with different sizes. Because it is not possible to foresee the size of the source before the reconstruction, in the future we will simultaneously estimate the value of p during the Lp-norm regularization from the measurement data.

References

[1] Plonsey R. Bioelectric phenonmena. New York: McGraw Hill, 1969.

[2] Rudy Y, Messinger-Rapport B. The inverse problem of electrocardiography: solutions in terms of epicardial potentials. Critical Reviews in Biomedical Engineering 1988; 16:215–268.

[3] Huiskamp G, Greensite F. A new method for myocardial activation imaging. IEEE Transactions on Biomedical Engineering 1997;44(6):443–446.

[4] Wang L, Zhang H, Wong K, Liu H, Shi P. Physiological-model-constrained noninvasive reconstruction of volumetric myocardial transmembrane potentials. IEEE Transactions on Biomedical Engineering 2010;57(2):296–315.

[5] He B, Li G, Zhang X. Noninvasive imaging of cardiac transmembrane potentials within three-dimensional myocardium by means of a realistic geometry aniostropic heart model. IEEE Transactions on Biomedical Engineering 2003;50:1190–1202.

[6] Nash M. Mechanics and Material Properties of the Heart using an Anatomically Accurate Mathematical Model. Ph.D. thesis, Univ. of Auckland, New Zealand, 1998.

[7] Wang L, Zhang H, Wong K, Liu H, Shi P. Electrocardiographic simulation on personalized heart-torso structures using coupled meshfree-bem platform. International Journal of Functional Informatics and Personalized Medicine 2009;2:175–200.

[8] Aliev R, Panfilov EV. A simple two-variable model of cardiac excitation. Chaos Solutions and Fractals 1996; 7(3):293–301.

[9] Physionet/computers in cardiology challenge 2007: Electrocardiographic imaging of myocardial infarction. `http://physionet.org/challenge/2007/`, 2007.

[10] Title LM, Iles SE, Gardner MJ, Penney CJ, Clements JC, Horacek BM. Quantitative assessment of myocardial ischemia by electrocardiographic and scintigraphic imaging. Journal of Electrocardiology 2003;36(Suppl):17–26.

[11] Cerqueira MD, Weissman NJ, Dilsizian V, Jacobs AK, Kaul S, Laskey WK, Pennell DJ, Rumberger JA, Ryan T, Verani MS. Standardized myocardial segmentation and nomenclature for tomographic imaging of the heart. Circulation 2002;105:539–542.